



# SRC 2022





# UNIVERSITY of HOUSTON

---

EARTH AND ATMOSPHERIC SCIENCES

35<sup>TH</sup> ANNUAL



**STUDENT RESEARCH CONFERENCE  
AND  
ALUMNI & INDUSTRY OPEN HOUSE**

---

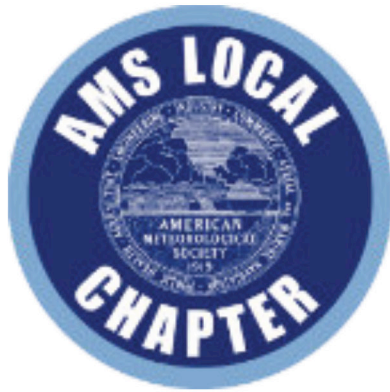
**APRIL 29, 2022**

---



# Table of **CONTENTS**

Schedule of Events .....	<b>1</b>
Oral Presentations .....	<b>2</b>
Session A.....	<b>2</b>
Session B.....	<b>4</b>
Poster Presentations .....	<b>6</b>
Keynote Speaker .....	<b>8</b>
Abstracts .....	<b>10</b>
Student Committee .....	<b>26</b>
Judges.....	<b>28</b>
Acknowledgements.....	<b>29</b>



*American Meteorological Society*  
UHStudentAMS@gmail.com



*AAPG Wildcatters*  
AAPG.Wildcatters@gmail.com



*GeoSociety*  
GeoSocietyatUH@gmail.com



*SEG Wavelets*  
SEGWavelets@gmail.com



*AEG @ AIPG*  
AEGatUH@gmail.com



# Schedule @ LOGISTICS

To join, click the Zoom Meeting ID of your choosing and enter the 6-digit passcode when prompted.

<b>ORAL SESSIONS</b>	9:00 am - 12:15 pm	935 4839 2560	336202
<b>INTERMISSION</b>	10:30 - 10:45 am		
<b>LUNCH BREAK</b>	12:15 - 1:00 pm		
<b>POSTER SESSIONS</b>	1:00 - 2:30 pm	952 2389 0402	373051
<b>INTERMISSION</b>	2:30 - 3:00 pm		
<b>KEYNOTE SPEAKER</b>	3:00 - 3:30 pm	935 4839 2560	336202
<b>AWARDS CEREMONY</b>	3:30 - 4:30 pm	935 4839 2560	336202
<b>HAPPY HOUR</b>	5:00 pm		

*Our happy hour is optional for all faculty, students, alumni, and industry members to join:*



2425 NORFOLK STREET  
HOUSTON, TX 77098

**9:00 AM**

*Tabitha Lee*

Identifying Unreported NO<sub>2</sub> Hotspots in Satellite Data

**9:15 AM**

*Claire Ong*

Analysis of PFAS in the Edwards Aquifer

**9:30 AM**

*Bavand Sadeghi*

Contributions of Meteorology to Ozone Variations: Application of Deep Learning and the Kolmogorov-Zurbenko Filter

**9:45 AM**

*Muhammad Nawaz Bugti*

Revised Plate Model for the Opening of the Gulf of Mexico Basin Based on a More Precise Definition of the Continent-Ocean Boundaries from Multiple Data Types

**10:00 AM**

*Veronica Guzman*

Stress Variations in the Delaware Basin from Shear-Wave Splitting Analysis

**10:15 AM**

*Md Nahidul Hasan*

Estimating Thermal Stress and Expelled Hydrocarbons from Mesozoic-Cenozoic Source Rocks of Southern Gulf of Mexico



**10:45 AM**

*Wei Li*

Spatial Variation of Surface O<sub>3</sub> Responses to Drought Over the Contiguous United States During Summertime: Role of Precursor Emissions and Ozone Chemistry

**11:00 AM**

*Ruby Patterson*

In Situ Resource Utilization Potential of Artemis Landing Site 105, Lunar South Pole

**11:15 AM**

*Chesney Petkovsek*

Mechanism to Explain Lateral Variations in the Geothermal Gradient of the Delaware Basin, West Texas, as Measured and Calibrated from 1,024 Deep Exploration Wells

**11:30 AM**

*Ali Mousavinezhad*

Investigation of Ground-Level Ozone Pollution in China, 2015–2019

**11:45 AM**

*Madeline Statkewicz*

Changes in Precipitation Patterns in Houston, TX

**12:00 PM**

*Ana Vielma*

Distribution of Trace Elements Inside Source Rocks

**9:00 AM**

*Nina Zamanialavijeh*

High-Velocity Slip During Thermal Decomposition of Carbonates: Example from the Heart Mountain Slide Ultracataclasites, Wyoming

**9:15 AM**

*Juan Pablo Ramos*

Coniacian-Santonian-Sourced Petroleum System along the Deepwater Caribbean Margin of Colombia

**9:30 AM**

*Kenneth Shipper*

Testing Rift Versus Transform Models for the Guyana Margin Using 3D Gravity Model in Contrast to Seismic Reflection Data

**9:45 AM**

*Michael Martinez*

Numerical Lithospheric Flexure in the U.S. Midcontinent: Towards an Assessment of Post-Laramide Uplift and Subsidence

**10:00 AM**

*Sara Rojas*

Quantifying Vegetation and Land Cover Changes about the Path of Hurricane Harvey

**10:15 AM**

*Mohamed Abdelfatah*

Crustal Structure of the Northwestern Red Sea Rifted-Passive Margin Based on an Integration of Seismic Refraction, Seismic Reflection, and Outcrop Data

**10:45 AM**

*Shihab Ahmad Shahriar*

Application of Deep Learning to Model Reference Crop Evapotranspiration (ET<sub>o</sub>) in Bangladesh

**11:00 AM**

*Tanzina Akther*

Ozone Precursors and Boundary Layer Meteorology Before and During a Severe Ozone Episode in Mexico City

**11:15 AM**

*Ellen Creecy*

Mars' Emitted Energy and Seasonal Energy Imbalance

**11:30 AM**

*Sharmila Appini*

Evaluating Intra-slab Anisotropy Using the Backazimuth Dependence of Shear Wave Splitting Patterns at West Pacific Subduction Zones

**11:45 AM**

*Daniella Easley*

Variations in the Expellable Potential of Late Cretaceous Source Rocks from Trinidad to Guyana: An Evaluation of the Influence of Tectonic, Paleogeographic, and Global Isotopic Excursions on Organic Deposition and Preservation

**12:00 PM**

*Masoud Ghahremanloo*

A Novel Deep Learning Model to Estimate Surface NO<sub>2</sub> levels from Remote Sensing Data: 15-Year Study Over the Contiguous United States

The poster sessions will take place during the afternoon from 1:00 PM – 2:30 PM.

**Morshad Ahmed**

*Sources of Atmospheric Nitrophenols in Houston*

**Lisabeth Arellano**

*Isotopic characterization ( $d_{18}O$ ,  $dD$ ,  $d$ -excess, and  $D'_{17}O$ ) of Panamanian rainfall to trace regional water cycling*

**Christopher Calvelage**

*Earth's wandering rotation axis influenced by mantle convection*

**Noelle Cheshire**

*The Association Between Texas PM<sub>2.5</sub> Density Distribution and Lung Cancer Statistics*

**Rachel Clark**

*Sediment transport and accumulation in the Amundsen Sea, West Antarctica*

**Leonardo Collier**

*Modelling Martian Fault Displacement through HiRISE Datasets*

**Michael Comas**

*Sedimentary Record of Recent Retreat of Pine Island Glacier, Amundsen Sea, Antarctica*

**Otto Gadea**

*Detection of Bastnäsite-Rich Veins in Rare Earth Element Ores through Hyperspectral Imaging*

**Presley Greer**

*GPR Imaging of permafrost in the CRREL Permafrost Tunnel, Fairbanks Alaska*

**Irfan Karim**

*Identifying anthropogenic methane emissions sources in University of Houston, Texas*

**James McConnell**

*Distribution and thickness of sediment-filled rifts in the deep-water Camamu-Alamada rifted-passive margin of northeastern Brazil*

**Muhammad Qasim**

*Integration of multispectral and hyperspectral remote sensing data for lithological mapping in Zhob Ophiolite, Western Pakistan*

**Kamil Qureshi**

*Structural Geometry and Lateral Propagation of the Surqamar Anticline, Northern Suleiman Fold-Thrust Belt, Western Himalayas*

**Steven Ramirez**

*Searching for slabs within the Earth's mantle through tomographic Analysis of the north Pacific Basin*

**Aydin Shahtakhtinskiy**

*Quantifying the impact of Hurricane Harvey on barrier island systems of the Central Texas Coast and their recovery: an example from Mustang Island*

**Larkin Spires**

*Observations from Empirical Fluid Substitution in Shales: Why Use the Voigt-Reuss-Hill Average?*

**Stephanie Suarez**

*Petrologic and Characterization of Olivine-Phyric Depleted Shergottites Northwest Africa 2046 and Northwest Africa 6162*

**Ozzy Tirmizi**

*Hazard Potential in Southern Pakistan: A Study on the Subsidence and Neotectonics of Karachi and Surrounding Areas*

**Luis Torres**

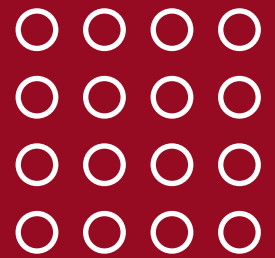
*The Influence of Basal Slip Plane Morphology on the McCartney structure*

**Faith Walton**

*Structural restoration of submarine and coalesced pull-apart basins in the northern Gulf of California*

Dr. Jonny Wu

**KEYNOTE SPEAKER**



**Un-subducting lost tectonic plates in Earth's mantle to rewind Deep Time**



**04.29.2022**

Assistant Professor  
Structural Geology, Tectonics,  
& Mantle Structure

<http://easd.geosc.uh.edu/wu/wordpress/>

**DR. JONNY WU** is UH Assistant Professor in structural geology, tectonics and mantle structure in the Department of Earth and Atmospheric Sciences. Wu is a Canadian and obtained his PhD at Royal Holloway, University of London, UK, followed by a postdoctoral fellowship at National Taiwan University. His research focuses on reconstructing Earth history by un-deforming folded and faulted geologic structures. In 2019 he received the National Science Foundation CAREER award to reconstruct the Panthalassa Ocean, a now-vanished ocean shrouded in mystery that once covered half of our planet during the time of dinosaurs.



Plate tectonics is the ‘grand unifying theory’ of Earth Science. Our knowledge of Earth’s past, including its climate, large-scale landmass movements, mantle circulation, spin axis movements, and other geologic phenomenon depend on inputs from plate tectonic reconstructions models. However, classic plate reconstructions permit less than half of Earth’s surface to be reliably reconstructed prior to Early Cretaceous times, which is only the most recent <3% of Earth history. The main barrier to rewinding Deep Time is the subduction and loss of oceanic plates into Earth’s mantle, which has consumed vital constraints including seafloor magnetic anomalies, hotspot tracks and geology.

In this keynote, I reconstruct Earth’s plate tectonic history by un-subducting lost oceanic plates in Earth’s mantle (i.e. slabs) from seismic tomography, which are medical CT scan-like images of the Earth’s interior. Subsurface mapping techniques borrowed from the energy industry are used to structurally restore the subducted plates back to the Earth surface. Our 4D jigsaw puzzle of restored tectonic plates provides new perspectives on large swaths of our planet during the Cenozoic and Mesozoic eras.

## UNDERGRADUATE GEOLOGY

### Noelle Cheshire

#### *The Association Between Texas PM<sub>2.5</sub> Density Distribution and Lung Cancer Statistics*

This project aims to draw parallels between fine particulate matter and fluctuating cancer rates in Texas state counties. PM<sub>2.5</sub> represents atmospheric pollutants such as NO<sub>x</sub>, VOC's, O<sub>3</sub>, SO<sub>2</sub>, etc. These pollutants are particularly dangerous due to their size which makes them easily distributed and consumed. PM<sub>2.5</sub> is also very dangerous because of the simple fact that only 18% of emissions occur naturally, thus unfortunately not only are we responsible for the other 82% of this pollutant but it's one that poses a huge health risk. This is why I believe it is so important to understand the correlation between anthropologic pollution and the effect they have on human health. In addition to determining cancer trends based on air quality, I also wanted to investigate if these two variables disproportionately affect different ethnic groups, specifically in metropolitan areas.

### Leonardo Collier

#### *Modeling Martian Fault Displacement through HiRISE Datasets*

Presently there is no numerical model for fault displacement on Mars; in this project we utilize HiRISE remote imagery and open-source GIS software to map and measure the relative displacement of faulting to develop the first comprehensive numerical model of these fault systems. Multiple elevation profiles and the overall length of the fault were mapped through a combination of JMARS and Google Earth Pro for each of the surveyed fault systems. Three discrete fault systems were surveyed across the planet's surface to build our model and we expect there to be a high degree of similarity to existing models on other rocky bodies. Developing a displacement model for Mars will better allow us to understand and interpret these fault systems and make better predictions of deformation on the red planet.

### Steven Ramirez

#### *Searching for slabs within the Earth's mantle through tomographic Analysis of the north Pacific Basin*

The reconstruction of subducted lithospheric plates is important to understand the behavior of current tectonic activity and its effect over long periods. Reconstruction uncertainty increases as we go farther back in time, reducing accuracy reconstructions of the subducted lithosphere. This study aims to construct a 3-D plate reconstruction model from detected fast-velocity, slab-like seismic anomalies under the North Pacific basin. Public seismic tomography data and 3-D spatial analysis were utilized to reconstruct the anomalies detected within the mantle. GOCAD, a petroleum industry mapping software, allowed for the construction of a working slab model from the analyzed tomographic data. The working model was entered into the open-software GPlates to observe how it filled out a previous plate reconstruction model and track its movement through time. The results showed that the slab interpretations correlated well with the conjugate reconstruction model to suggest past intra-oceanic subduction before 125 Ma within the Pacific Basin. Raw tomographic data supported the identified area of slab subduction from the Izanagi plate occurring before 125 Ma. Slab reconstruction demonstrated a connection with the Koyukuk accreted terrane of western Alaska. The Koyukuk terrane is interpreted to have collided with the North American plate margin around the Late Cretaceous. Age dating of granitic plutons and the collision timing suggest an origin due to intra-oceanic subduction around 175-155 Ma. The Koyukuk terrane was used as a reference to create a maximum size plate model for a newly proposed 'Koyukuk plate'. Further research is necessary to determine more precise constraints of the Koyukuk plate, but our model provides a new tectonic connection between the mantle and Alaskan geology to inspire future studies.

### Luis Torres

#### *The Influence of Basal Slip Plane Morphology on the McCartney structure*

The formation of salient geometries in thrust belts has been explored and explained through several different processes. However, the influence of basal slip plane morphology has so far received limited attention as an additional mechanism to produce curved thrust-fold belts. In several orogens, the basal thrust geometry is far from being a simple plane and shows ramps, lateral ramps and other geometrical complications. We propose to explore this possibility with a simple analog deformation experiment including a buttress of known morphology, coupled with a control experiment without any buttress. In order to do this, a 2x3 foot rig with an orthogonally moving back wall used to simulate compression was built. The initial reference experiment consisted of a sand pack of approximately 65 cm x 50 cm x 2.5 cm, with a 2 cm layer of white sand and a 0.5 cm layer of pink sand. This sand pack was placed above a flat, smooth surface wrapped in PTFE tape to reduce the friction and was then pushed by the backwall in an eastern direction. The buttress experiment consisted of a sand-pack of 65 cm x 50 cm x 2.25 cm, it had a 2 cm layer of white sand and a 0.25 cm layer of pink sand. The sand-pack was placed over a smooth surface with a buttress located 36.5 cm away from the back wall. Through the first 21 cm, both experiments develop similarly with several parallel imbricated thrusts. At 21.5 cm of shortening a curved and more centralized fault began to form as a result of the sand-pack interacting with the buttress. This fault, unlike the others did not propagate across the entire sand-pack. As the shortening continued, the major faults continued to form in the central part of the buttress with several closely spaced faults forming toward the outside of the model. The buttress model also showed the development of two symmetrical lateral ramps that accommodated for the resistance caused by the buttress. With the introduction of a buttress a salient was developed similar to that of the Helena salient and McCartney Mountain salient.



### **Faith Walton**

#### *Structural restoration of submarine and coalesced pull-apart basins in the northern Gulf of California*

The enclosed marine seaway of the Gulf of California between mainland Mexico and the Baja Peninsula opened during a period of Late Miocene (12.5 Ma) to Recent transtension along the right-lateral San Andreas Fault system that separates the North American and Pacific plates. The 187 km-wide marine area of the northwestern Gulf of California overlies two, now coalesced, thickly-sedimented pull-apart basins: a 5 km-wide, right step in the right-lateral Amado and Tiburon-La Cruz fault zones produced the 3,042 km<sup>2</sup> Adair-Tepoca and Upper Tiburon rhomboidal pull-apart basins in the north; in the south a 60-km-wide, right-step in the right-lateral Cerro Prieto and Ballenas fault zones produced the 5,960 km<sup>2</sup> Wagner-Consag and Upper-Lower Delfin rhomboidal pull-apart basins. The northern pull-apart basin was active during the period of 6 Ma and was abandoned by 3.3-2 Ma while the southern pull-apart basin is thought to have been initiated by 3 Ma and remains active to the present day based on seismic reflection and the linear alignments of earthquakes. The two basins of different ages have coalesced into a single, large marine depocenter that are separated by a narrow ridge of basement rocks that includes Angel de la Guarda Island. In this study I structurally restore the entire depocenter by using three independent methods: 1) Matching bedrock outcrops of pre-rift, Miocene tuffs and restoring them to a continuous geometry now present on the conjugate margins of the Gulf of California; matched units include the well dated San Felipe and Mesa Cuadrada formation of 12.5 Ma and 6.5 Ma age respectively; this method yields a total of 250 km of offset; possible errors are large as these outcrops are at the coastline and could extend further seaward; offsets on subaerial strike-slip exhibit a total right-lateral offset of 5 km that is known from dating of the offset units; and 2) A full-fit reconstruction of the underlying, stretched continental crust that is known from previous seismic refraction studies to range in thickness from 30 to 15 km with a small intervening area of oceanic crust.

## **UNDERGRADUATE GEOPHYSICS**

### **Presley Greer**

#### *GPR Imaging of permafrost in the CRREL Permafrost Tunnel, Fairbanks Alaska*

Permafrost is a term that refers to the ground which remains at or below 0 degrees Celsius for two or more years. There tend to be three layers to permafrost; the active layer is the topsoil layer which freezes in the winter and then thaws in the summer; the permafrost table is the upper surface of the permafrost, which changes temperature throughout the seasons; isothermal permafrost is the region of permafrost that has no variation in temperature throughout the seasons. There have been recent changes in northern Alaskan permafrost due to changes in the climate and temperature rises causing the active layers to expand vertically resulting in the permafrost table melting. Within the permafrost, there are ice wedges which developed from the expansion of water freezing and displacing the surrounding soil. As these wedges of ice melt, empty cavities begin to form within the soil below. After these cavities collapse, they're referred to as thermokarst sinkholes. These sinkholes have been known to form within Fairbanks as well as other places in Alaska and have caused damage to the infrastructure. Further thermokarst formations threaten to develop with the ever-changing climate, so monitoring permafrost in the subsurface is vital to understanding and mapping areas with the potential of developing into future thermokarst sinkholes. Future developments of thermokarst sinkholes could potentially cause damage to highways, buildings, and possibly the Alaskan pipeline. To better understand these changes in the permafrost and the associated risks, a survey was carried out in multiple steps using both GPR data and visible/thermal camera data from a UAS. This survey used a 200 MHz, 400 MHz, and a UAS with a visible-thermal camera combo. Precambrian schist was mapped along with some layers of gravel, silt, sand, and some ice wedges. This data is intended to be built upon in the future with other surveys for the continued monitoring of permafrost layers.

## MASTERS GEOLOGY

### Michael Comas

#### *Sedimentary Record of Recent Retreat of Pine Island Glacier, Amundsen Sea, Antarctica*

Pine Island Glacier (PIG), which terminates in the Amundsen Sea Embayment (ASE), has been recently identified as the single-largest contributor to global sea-level rise from Antarctica. This is believed to be a result of changes in climate in the Amundsen Sea and the nearby Southern Ocean. Oceanographic sampling in, and models of, the ASE have found that slightly warmer Circumpolar Deep Water (CDW) has been incuring onto the continental shelf as a response to strengthening winds in the region. The continental shelf in West Antarctica has a reverse-sloping bed topography which was carved after repeating cycles of glaciation, and provides avenues for the denser CDW to travel down-slope and reach the grounding line of glaciers terminating in the ASE. The exact timing of the first incursions of CDW onto the shelf of the ASE is unknown; however, since the beginning of satellite data acquisition, PIG has been experiencing ice shelf thinning and grounding line retreat. Preliminary investigation into the recent history of PIG has shown that its initial retreat may have been triggered in the mid 1940's. This study seeks to provide a detailed and larger-scale understanding of PIG's dynamics by investigating properties of sediments collected proximal to PIG. Sediments cores were collected in 2020 from newly-exposed seafloor immediately following the calving of a large portion of Pine Island Ice Shelf. Initial core descriptions suggest that the retreat of PIG's grounding line may have been preserved where very poorly sorted diamicts (sub-glacial) are overlain by finer-grained, well-sorted sediments (glacial-marine). To determine the timing of these changes in environment, grain-size and grain-shape analysis will be conducted alongside radio-isotopic dating methods. Measurements of  $^{210}\text{Pb}$  within the sediments and  $^{14}\text{C}$  from foraminiferal tests allow for the construction of age models to establish timing and rates of sediment deposition in the area. Determining the timing and pace of the initial retreat of PIG will aid in the constraining of models of PIG's dynamics which is a crucial step in preparing for global sea-level rise in the near future.

### Michael Martinez

#### *Numerical lithospheric flexure in the U.S. Midcontinent: towards an assessment of post-Laramide uplift and subsidence*

The Cenozoic history of the central U.S. is characterized by widespread marine regression and uplift following the ending of the Laramide orogeny and the Western Interior Seaway, implying a long-term decrease of accommodation space. The precise history of uplift through space and time, however, and its dynamic causes, are not well known. The Cretaceous-Paleocene sequence of marine sediments is capped, after a significant unconformity, by the Late Miocene Ogallala Formation, which is comprised of eolian and fluvial sands and gravel derived from the uplifted ranges to the West of this study area. This suggests a phase of subsidence, or at least a lull in regional uplift. The post-depositional history of the Ogallala formation, however, is characterized by tilting and uplift, as shown by paleoslope studies of the Ogallala formation (McMillan et al., 2002; Pattat et al., 2017). These observations are tentatively connected to several ongoing processes, such as the opening of the Rio Grande Rift, the flexural unloading induced by erosion of the Rocky Mountains and the High Plains, and far-field stresses coming from plate boundaries and from the deep mantle. In this talk, I will focus on the role of flexural isostasy using a finite difference model and try to assess whether flexural unloading alone can satisfactorily explain the observed Miocene-Present uplift in the U.S. Midcontinent. Building on previous paleoslope work, I will investigate flexure rigidity controls on lithospheric deflection and compensation along two regional transects and then share some outlook as to how I can use my model to investigate the uplift and tilting history of the Ogallala Formation as a function of strength of the lithosphere through time.

## MASTERS GEOPHYSICS

### Sharmila Appini

#### *Evaluating intra-slab anisotropy using the backazimuth dependence of Shear Wave Splitting patterns at west pacific subduction zones*

It has been shown that many deep subduction earthquakes (whose depth  $> 60$  km) show large non-double couple components (ndcc) in the results of moment tensor analyses. These findings are used as proof to argue that deep earthquake mechanisms are different from shallow earthquakes. Recently, it was shown that there is strong evidence of high seismic anisotropy in the vicinity of deep earthquakes (subducting slabs) which can cause the observed apparent ndcc. If this hypothesis is correct, an important consequence is that the strong anisotropy in the dipping slabs can cause the observed different shear wave splitting (SWS) patterns which critically depend on the back-azimuths of earthquakes as well as the slab anisotropy. It is in sharp contrast with many previous SWS studies which did not consider the source locations in the interpretation. We will evaluate this hypothesis in the Japan subduction zone, using Hi-net stations ( $>760$ ) for global earthquakes. The preliminary results obtained from 400 stations located in Japan and 460 teleseismic earthquakes located mainly in Java and Tonga, suggest a variation of the delay time between the fast and slow S waves from about 0 sec to  $\sim 3$  sec. Both the fast S polarization and the delay time have a complex relation with respect to the source location and epicentral distance. These measurements will be further used to test if a tilted transverse isotropy slab can cause the SWS observations using 3D-anisotropic elastic finite difference modeling and a propagator matrix method. It is expected that an intra-slab anisotropic model can simultaneously explain both the earthquake ndcc radiation patterns and the observed SWS patterns.

## Ph.D. ATMOSPHERIC SCIENCE

### Morshad Ahmed

#### *Sources of Atmospheric Nitrophenols in Houston*

Nitrated phenols (NPs) are compounds that comprise hydroxyl- and nitro- functional groups attached to the benzene rings. Primary sources of NPs include vehicle exhaust, waste incineration plant, biomass burning emissions and secondary NPs and their derivatives (e.g. methyl NPs) can be formed by the gas-phase reaction of OH or NO<sub>3</sub> radicals in presence of NO<sub>2</sub> with various aromatic precursors. During the Study of Houston Atmospheric Radical Precursors (SHARP) campaign NPs including 2,4-DNP, 4-NP, 2-NP, and 2-Me-4-NP and comprehensive atmospheric chemistry data set were measured hourly at the Moody Tower (MT) site (29.7172° N, 95.3416° W), Houston, Texas from May 15 to June 30, 2009. The SHARP NP data for Houston shows maximum concentrations for 4-NP, followed by 2-Me-4-NP, 2-NP, and 2,4-DNP which might indicate rapid photochemistry. NP concentrations in Houston were found to be higher compared to other studies conducted in summer and comparable with studies conducted in winter. Source apportionment of NPs and other atmospheric pollutants (i.e., volatile organic compounds, SO<sub>2</sub>, CO) is conducted based on Positive Matrix Factorization (PMF) which yielded nine factors: secondary formation (21.9%), nitrophenols source (4.1%), petrochemical industries/oil refineries (10.4%), monoterpenes (5.4%), traffic (14.3%), biogenic (4.3%), phenol source (2.3%), naphthalene source (2.3%), and natural gas/crude oil (24.9%). Bivariate polar plots suggest that the Houston Ship Channel and oil refineries are the primary emission source for petrochemical industries/oil refineries, monoterpenes, phenol, naphthalene, and natural gas/crude oil sources. The Nitrophenols source showed a diverse pattern that needs to be investigated further. Future research will focus on the understanding of the formation of secondary NPs, their impact on HONO formation, and OH production using AtChem2 Master Chemical Mechanism (MCM) v3.2 box model in an urban area with complex emission sources, here in Houston.

### Tanzina Akther

#### *Ozone precursors And Boundary Layer Meteorology Before and During a Severe Ozone Episode in Mexico City*

Volatile organic compounds (VOCs) data in conjunction with other inorganic pollutants, surface meteorological data and continuous measurement of the Planetary Boundary Layer height (PBLH) at an urban site in Mexico City were performed from 6 to 18 March 2016. Positive Matrix Factorization (PMF) identified four emission source factors: (1) secondary aerosol, (2) evaporation and non-LPG fuel combustion (3) geogenic source and (4) vehicle exhaust. Propylene Equivalent and Maximum Incremental Reactivity (MIR) methods identified isoprene and ethylene as the highest oxidation and O<sub>3</sub> forming species. Pollutant data normalized to the variation of the planetary boundary layer height (PBLH) revealed continued emissions of O<sub>3</sub> precursors in the afternoon beyond the typical morning rush hour. In particular this could be observed during the second part of the measurement period (12-15 March) when a strong O<sub>3</sub> episode occurred under weak wind and lower PBLH conditions compared to the preceding period (6-11 March) when well mixed conditions due to elevated daytime PBLH and strong advection led to overall reduced pollutant mixing ratios in the afternoon hours.

### Ellen Creedy

#### *Mars' Emitted Energy and Seasonal Energy Imbalance*

The radiant energy budget of a planet is essential to understanding its surface and atmospheric processes. Here, we report the first systematic measurements of Mars' emitted power, which are used to estimate the radiant energy budget of the red planet. Based on the observations from Mars Global Surveyor, Curiosity, and InSight, our measurements suggest that Mars' global-average emitted power is  $111.7 \pm 2.4$  Wm<sup>-2</sup>. More importantly, our measurements reveal strong seasonal and diurnal variations of Mars' emitted power. The strong seasonal variations further suggest an energy imbalance at the time scale of Mars' seasons (e.g., ~ 15.3% of the emitted power in the Northern autumn for the Southern Hemisphere), which could play an important role in generating dust storms on Mars. We also find the 2001 global dust storm decreased the global-average emitted power by ~22% during daytime but increased the global-average emitted power by ~29% at nighttime. This suggests that global dust storms play a significant role in Mars' radiant energy budget.

**Masoud Ghahremanloo***A Novel Deep Learning Model to Estimate Surface NO<sub>2</sub> levels from Remote Sensing Data: 15-Year Study Over the Contiguous United States*

This study proposes a novel two-step deep learning (DL) model to estimate surface NO<sub>2</sub> concentrations at 7×5.5 km spatial resolution over the contiguous United States (CONUS) from 2005 to 2019. The first phase of the model uses a partial convolutional neural network (PCNN), an advanced DL model, to accurately impute the gaps between surface NO<sub>2</sub> stations, and create 5,478 daily-mean NO<sub>2</sub> grids (PCNN-NO<sub>2</sub>) in the 2005-2019 period over the study area. In the second phase of the model, the PCNN-NO<sub>2</sub> along with other predictor variables are fed into a deep neural network (DNN) to estimate surface NO<sub>2</sub> levels, achieving exceptional performance with an R of 0.975 to 0.978, MAB of 0.99 ppb to 1.38 ppb, and RMSE of 1.47 ppb to 1.97 ppb. The spatial-CV results also indicate the high spatial performance of PCNN-DNN at surface NO<sub>2</sub> estimation. In addition to high estimation accuracy, the PCNN-DNN model generates consistent estimated NO<sub>2</sub> grids without any missing values, improving the quality of various applications, such as emission reduction strategies and public health studies. The 5,478 daily estimated NO<sub>2</sub> grids, between 2005 and 2019, over the CONUS reveal significant reductions in NO<sub>2</sub> levels in fourteen major urban environments — Washington DC (-43%), New York (-45%), Los Angeles (-38%), Chicago (-25%), Boston (-43%), Houston (-34%), Dallas (-40%), Philadelphia (-41%), Phoenix (-38%), Detroit (-20%), Denver (-23%), Atlanta (-0.7%), Cincinnati (-38%), and Pittsburgh (-56%).

**Irfan Karim***Identifying anthropogenic methane emissions sources in University of Houston, Texas*

Methane (CH<sub>4</sub>) is a significant greenhouse gas in the atmosphere, can be formed through thermogenic or biogenic processes. Identifying CH<sub>4</sub> emissions is important to understanding potential impacts of various anthropogenic sources in the vicinity of University of Houston. The determination of carbon isotope ratios of CH<sub>4</sub> ( $\delta_{13}CCH_4$ ) have been effective technique for segregating individual CH<sub>4</sub> sources. Measurements of CH<sub>4</sub> and ( $\delta_{13}CCH_4$ ) were performed with cavity ring-down spectrometer (CRDS) at the Moody Tower. CH<sub>4</sub> distributions and the  $\delta_{13}CCH_4$  signatures were obtained from November 1st, 2021 to April 17th, 2022. Measurements indicate higher CH<sub>4</sub> concentrations (2.3 – 2.5 ppm) with winds from N-NE between 2-4 m/s-1. This coincides with the McCarty landfill site, which is located ~15 km northeast of the sampling location. Results highlight that the variations in the day-night CH<sub>4</sub> and  $\delta_{13}CCH_4$  concentrations were affected by the diurnal variations of both the emission intensity and atmospheric processes

**Tabitha Lee***Identifying Unreported NO<sub>2</sub> Hotspots in Satellite Data*

Nitrogen oxides (NO<sub>x</sub>) are influential in atmospheric chemical reactions and can negatively affect the health of a population. Yet, because of their abundant sources and short lifetime, not all emission events are indicated by bottom-up emission inventories or seen by sparse in situ measurements. Satellite instruments (e.g., TROPOMI 3.6x5.6 km<sup>2</sup> at nadir) have the potential of capturing unreported emission events through the observation of high NO<sub>2</sub> signals. Previous studies have shown the importance of unreported emission events but have used inefficient methods for identify these events. To the best of our knowledge, there is no standard method to identify unreported emission events. A suitable algorithm is needed to screen through a vast amount of satellite data to identify 'unreported' hotspots. Clustering algorithms resolves obstacles for identification as this data mining method allows for the detection of NO<sub>2</sub> signals by grouping the signals based on their similarity. This class of algorithms allows for different magnitudes of signals to be discovered and grouped together which reveals emission event. The difficulty of applying a clustering algorithm to satellite observations arise from two issues: the size of data observations and the coupling of the spatial and temporal properties in satellite observations. Many popular clustering algorithms are inefficient in capturing the spatial and temporal attributes of satellite observations as the two attributes are infrequently addressed in combination. In this study we apply different clustering algorithms to TROPOMI observations and suggest an alternative process to identify potential unreported emission events. We conduct tests on two areas in Texas where potential unreported emission events have been identified. A range of parameters that factor into the classification of an unreported emission event, including distance to a known emission source, frequency, and potential emission source, are studied. We further use the identification results to aid in the standardization of identifying unreported emission events in satellite observations.

**Wei Li***Spatial Variation of Surface O<sub>3</sub> Responses to Drought Over the Contiguous United States During Summertime: Role of Precursor Emissions and Ozone Chemistry*

Drought is an extreme weather and climate event that has been shown to cause the worsening of ozone (O<sub>3</sub>) air pollution. Using 15-year (2005-2019) surface O<sub>3</sub> observations and weekly US Drought Monitor (USDM) indices, this study estimated that summertime US-mean surface O<sub>3</sub> increased by 1.47 ppb per USDM level. It is revealed that O<sub>3</sub> responses to drought display a spatial east-west variation: higher O<sub>3</sub> enhancement in the Southeast (2.24 ppb/USDM), and no significant change or even a decrease in the west (e.g., -0.06 ppb/USDM in California). The diurnal changes of O<sub>3</sub> with drought also show an opposite pattern between the Southeast and California. Formaldehyde (HCHO) and nitrogen dioxide (NO<sub>2</sub>) column, two satellite-based O<sub>3</sub> precursors proxies, show an increasing rate of 0.41 x10<sup>15</sup> molec/cm<sup>2</sup>/USDM and 0.03 x10<sup>15</sup> molec/cm<sup>2</sup>/USDM in the Southeast, respectively, while these rates are not statistically significant in California. We explained this spatial discrepancy from the perspective of O<sub>3</sub> chemistry by applying a zero-dimensional model at the sites with long-term observations in California and Georgia. Isoprene concentrations decreased by ~37% under exceptional drought in California causing a reduction of O<sub>3</sub> production (PO<sub>3</sub>) by ~23.7% during daytime. On the contrary, isoprene increased by ~41% in Georgia inducing a consequent increase of PO<sub>3</sub> by ~33.4% which accounts for more than half of the O<sub>3</sub> enhancement. This study reveals the key role of biogenic isoprene on ozone chemistry under drought conditions.

**Ali Mousavinezhad***Investigation of ground-level ozone pollution in China, 2015–2019*

Despite the considerable reductions in primary and secondary air pollutants in China, surface ozone levels have increased in recent years. We report a trend of  $3.3 \pm 4.7 \mu\text{g}\cdot\text{m}^{-3} \text{ year}^{-1}$  in the annual mean maximum daily average ozone over an 8-h period (MDA8 ozone) across China between 2015 and 2019. Leveraging the Kolmogorov–Zurbenko filter method, we find that meteorology enhanced the ozone levels in Beijing–Tianjin–Hebei (BTH), the Yangtze River Delta (YRD), and the Pearl River Delta (PRD) while the reduction of solar radiation and the planetary boundary layer height accelerated ozone decreases in the Sichuan Basin (SCB) after 2017. Solar radiation and temperature increases, together with the reduction in sea level pressure, were the main contributors to enhance ozone in the YRD. They also contributed to 32% of ozone increases in BTH. Weaker meridional wind, lower relative humidity, and higher temperature escalated ozone enhancement in the PRD between 2016 and 2018. Regarding precursor emissions, NO<sub>2</sub> long-term components showed a noticeable decline in all regions after 2017, partially due to the introduction of the most current action plan to reduce air pollutants over China in 2018. In contrast, the satellite-retrieved data suggest that VOC concentrations did not change substantially in target regions during the study period. After 2017, however, VOCs slightly increased in BTH, the YRD, and the PRD, which might be driven by temperature enhancements. Overall, the impact of meteorology on ozone variations was dominant in the YRD, the PRD, and the SCB from 2015 to 2019. Precursor emissions, however, played a leading role in ozone enhancement over the BTH. We also found that BTH and the YRD were in a transitional ozone formation regime while the PRD and the SCB tended to be more NO<sub>x</sub>-sensitive.

**Bavand Sadeghi***Contributions of meteorology to ozone variations: Application of deep learning and the Kolmogorov-Zurbenko filter*

From hourly ozone observations obtained from three regions, Houston, Dallas, and West Texas, we investigate the contributions of meteorology to changes in surface daily maximum 8-hour average (MDA8) ozone from 2000 to 2019. We apply a deep convolutional neural network and Shapely additive explanation (SHAP) to examine the complex underlying nonlinearity between surface ozone and meteorological factors. Results of the models show that between 2000 and 2019, specific humidity (26% and 23%) and temperature (19% and 21%) contributed the most to ozone formation over the Houston and Dallas metropolitan areas, respectively. On the other hand, the results show that solar radiation (38%) strongly impacted ozone variation over West Texas during this time. Using a combination of the Kolmogorov-Zurbenko (KZ) filter and multiple linear regression, we also evaluate the influence meteorology on MDA8 ozone and quantify the contributions of meteorological parameters to trends in surface ozone formation. Our findings show that overall, long-term variations of meteorologically-independent ozone over Houston and Dallas decrease at a linear annual rate of  $0.19 \pm 0.016$  and  $0.22 \pm 0.019$  ppb, respectively. In West Texas, we observe a change of 0.06 ppb/yr for meteorologically-independent ozone. The results of this study showed SHAP analysis and the KZ approach can investigate the contributions of the meteorological factors on ozone concentrations and help the policymakers to enact effective ozone mitigation policies.

### Shihab Ahmad Shahriar

#### *Application of Deep Learning to Model Reference Crop Evapotranspiration (ET<sub>o</sub>) in Bangladesh*

ET<sub>o</sub> is an essential component of the hydrological cycle, and its assessment is needed for drought prevention and management. The Food and Agricultural Organization-derived Penman Monteith (FAO56PM) system is the most widely used reference model for calculating ET<sub>o</sub>. However, one significant disadvantage of this model is that it necessitates a large climatic dataset. Several experiments also promoted the usage of artificial intelligence to overcome this weakness. As a result, this thesis conducted a comprehensive literature review on the use of machine learning for estimating ET<sub>o</sub>, as well as an assessment of recently recognised deep learning models, in order to fill gaps and find an alternative to FAO56PM for Bangladesh. In 94 chosen trials, the average influence of the models in terms of precision was 0.88, according to the systematic literature review. The narrative synthesis of the literatures revealed three main gaps: no standard machine learning models, insufficient research on deep learning models, and the use of more than six weather parameters. This thesis compared three deep learning models, DeepAR, LSTM-AE, and Bi-LSTM-AE, to three classical machine learning models, ANN, SVM, and GPR to calculate ET<sub>o</sub>. The climatic parameters were collected from Bangladesh Meteorological Department (BMD) from 1980-2019 and estimate the ET<sub>o</sub> utilizing FAO56PM method. Then, Shapley Game Theory was used to determine the most influential features and feed them into the models. Sunshine hour (SH), wind speed (WS), and maximum temperature (Tmax), and relative humidity (RH) were the most influential influences for the stations. The climatic data (1980-2019) was divided into two parts: training data (80%) and testing data (20%). DeepAR outperformed all other versions with lower RMSE (0.08-0.23 mmd<sup>-1</sup>) and MAE (0.09 – 0.19 mmd<sup>-1</sup>) during test phase of the model implementation. As a result, the analysis recommends DeepAR as an alternate model to FAO56PM.

### Madeline Statkewicz

#### *Changes in Precipitation Patterns in Houston, TX*

There has been an alarming increase in the frequency of major flooding events along the Gulf Coast over the last three decades, primarily due to events of unprecedented, or extreme, rainfall. Using data from 63 rain gauges maintained by the Harris County Flood Control District's Flood Warning System (HCFCD FWS), this study examines the changes in daily precipitation amounts in the highly urbanized city of Houston, Texas, USA. The potential shift in annual precipitation patterns over a period of three decades (1989-2018) was examined by investigating the numbers of dry and wet days as well as annual precipitation totals over the study period. Wet days were then further scrutinized based on daily rainfall amounts (e.g., R10, R20, R30, R40, R50, R100) to determine if extreme events are beginning to dominate annual rainfall amounts. Trends were analyzed for statistical significance temporally using the Mann-Kendall and Sen's slope methods and for spatial trends using GIS applications. The results indicate a statistically significant increase in extreme rainfall at the expense of light, moderate, and heavy rainfall over time. The only negative relationship is found in dry days. The most statistically significant trends exist in the 99th percentile, maximum, and R100 parameters with p-values of 0.07, 0.08, and 0.11, respectively. There has been rapid growth and intensive development in the Houston area in recent decades that continues to this day, and land cover change has been significant as 15.2% of Harris County changed to one of four National Land Cover Database (NLCD) Urban classes (e.g., developed: barren, low intensity, medium intensity, high intensity). This confirms that urbanization has continued to increase while total vegetative and wetland coverage has decreased. The findings of this study provide essential guidance for city and state planners and engineers.

## Ph.D. EARTH SCIENCE

### Stephanie Suarez

#### *Petrologic and Characterization of Olivine-Phyric Depleted Shergottites Northwest Africa 2046 and Northwest Africa 6162*

Acquiring geochemical data from Martian specimens, whether from meteorites or returned samples, is essential in understanding the evolution of Mars. Shergottites, the most abundant class of martian meteorites, can provide information about early planetary differentiation, evolution of mantle reservoirs, and magmatic processes that occur in the crust and upper mantle. Northwest Africa (NWA) 6162 is characterized as an olivine-phyric depleted shergottite that was found in 2010 near Lbirat, Morocco. Northwest Africa (NWA) 2046 is categorized as an olivine-orthopyroxene-phyric shergottite that was found in near Labkhbi, Algeria in 2003. These two specimens belong to a suite of at least 16 olivine-phyric shergottites that are derived from incompatible trace element depleted sources and share a 1.1 Ma ejection age. This suite is hypothesized to represent an igneous succession on Mars, that possibly originated from the Tooting crater. By using comparative petrology on these specimens, we can investigate the potential diversity of emplacement environments recorded in the igneous pile. We present constraints on the petrogenetic histories of these specimens and compare them with other olivine-phyric shergottites that did and did not share a common ejection event. Polished thin sections of NWA 6162 and NWA 2046 were prepared for this study. A JEOL 7600F analytical field-emission SEM was used to obtain elemental maps for initial characterization at NASA Johnson Space Center, followed by quantitative spot analyses using a JEOL JXA-8900 EPMA at the University of Nevada, Las Vegas. Acquired textural and chemical data of pyroxenes from NWA 2046 and NWA 6162 suggest they have distinct thermal histories. The apparently more slowly cooled NWA 6162 and its cumulate texture may suggest this specimen may be derived from a sill or thick flow. Despite having an olivine-phyric texture, pyroxene and olivine compositions of NWA 6162 are similar to enriched poikilitic shergottites, but tend to be more homogeneous. Pyroxene compositions from NWA 2046 are consistent with other launch paired olivine-phyric shergottites including NWA 5789.

## Ph.D. GEOLOGY

### Mohamed Abdelfatah

*Crustal structure of the northwestern Red Sea rifted-passive margin based on an integration of seismic refraction, seismic reflection, and outcrop data*

Most continental rifts are Mesozoic in age and deeply-buried beneath 10-15 km of Mesozoic and younger passive margin sedimentary rocks. The Red Sea Oligocene to Recent in age, is shallowly buried, and exhibits minimal oceanic spreading that together allow detailed comparisons of the crustal structure of its conjugate rifted margins and its salt-filled sag basin and its thin passive margin section. In this study, I combine interpretations of previous refraction data; my own interpretation of an industry of 160 line-km; my own 2D gravity modeling based on publicly-available satellite data; previous refraction studies in the area; and previous outcrop data from the well-exposed bedrock margins of the rift. Using this integrated dataset, I construct two, parallel, 80-km-long, dip-oriented, crustal transects crossing the northwestern Red Sea margin. Both transects are extended 90 km inland from the shoreline of the northwestern Red Sea and provide excellent outcrop data from this part of the necking zone. The main results of the study include the following: 1) Integrated gravity and seismic data analysis reveal a 30-64 km wide necking domain that is underlain by a 10-30-km, thinned continental crust; 2) Evaporitic sequences of 1-7 km in thickness are generally deposited in post-rift sag basins that overlie half-grabens in the rifted, continental crust of the necking domain; in Egypt the necking domain is observed to lie both onshore and offshore with as much as 10-40 km of the necking domain located onshore in eastern Egypt; 3) The thickness of the salt layer that ranges from 1 to 5 km and mainly exhibits vertical diapirism related to the load of the thin, overlying passive margin section; and 4) the lithologies, thickness, and facies of pre-salt source and reservoir units of the central Red Sea can all be inferred from the pre-rift and syn-rift exposed outcrops of the necked zone in Egypt.

### Lisabeth Arellano

*Isotopic characterization ( $d_{18}O$ ,  $dD$ ,  $d$ -excess, and  $D^{17}O$ ) of Panamanian rainfall to trace regional water cycling*

The application of stable isotopes in hydrologic and paleoclimate studies entails an understanding of controls on modern precipitation variations, but such insight is complicated in tropical mountainous regions by the combined influence of orographic effects, microclimates, and moisture recycling. We present new  $d_{18}O$ ,  $dD$ ,  $d$ -excess, and  $D^{17}O$  values of tap samples from 35 sites and monthly precipitation samples from one site in Panama. Tap water values of  $d_{18}O$  range from -11.6 to -2.4‰,  $dD$  from -82.3 to -14.3‰,  $d$ -excess from 4.3 to 12.7‰, and  $D^{17}O$  from -8 to 84 per meg.  $d_{18}O$  decrease with distance from the Caribbean Sea and are correlated with site latitude, elevation, and mean annual precipitation, indicating  $d_{18}O$  patterns may be explained by progressive rainout of Caribbean-sourced moisture as air masses traverse the cordillera.  $D^{17}O$  do not show spatial trends or correlate with local environmental factors.  $D^{17}O$  are smallest in the country's interior and along the Colombian border, where Caribbean and Pacific-sourced waters with different  $d_{18}O$  may be mixing during the rainy season.  $D^{17}O$  are largest in Eastern Panama and inland near the Costa Rican border, suggesting precipitation in these areas experience short trajectories from oceanic sources and/or is sourced by recycled moisture. Monthly  $d_{18}O$  at Bajo Cedro range from -7.6 to 0.4‰ and are lower during the rainy season, correlated with average monthly precipitation indicating the prevalence of a temporal amount effect. An 18 per meg difference was observed between rainy and dry season  $D^{17}O$ , possibly due to lower moisture source relative humidity. Future work will improve interpretations by constraining effects of moisture source and rainfall type.

### Muhammad Nawaz Bugti

*Revised plate model for the opening of the Gulf of Mexico basin based on a more precise definition of the continent-ocean boundaries from multiple data types*

I re-define the continent-ocean boundaries (COB) of the conjugate, rifted margins of the Gulf of Mexico basin using the gravity field from satellite mapping, magnetic surveys, deep-penetration grids of 2D seismic reflection data, seismic refraction surveys, and heatflow measurements. This re-defined COB was then used as a basis for quantitative plate model for the Late Triassic-earliest Cretaceous opening history of the basin with these main phases: 1) Late Paleozoic-early Triassic closed fit with the Yucatan margin restored to the northwest against the area of the Appalachian-Ouachita and northeast-trending, subsurface rifts aligned between western Florida and the Yucatan Peninsula; 2) Middle to Late Jurassic, rifting of continental crust of the northern and southern GOM occurred from Late Triassic to Middle Jurassic with thinner crust resulting in a thermally-controlled sag basin filled with the Louann and Campeche salt of Bajocian age; 3) Oceanic spreading initiated during the Middle Jurassic with the formation of a single marginal rift that was localized thicker salt; the marginal rift was split into two by the oceanic spreading ridge so half of the marginal rift is found on the northern rifted margin and the other half is on the southern rifted margin; and 4) Middle Jurassic-earliest Cretaceous oceanic spreading along a single spreading ridge produces a prominent asymmetry in the oceanic crust with a broader zone of oceanic crust north of the ridge; a single pole of plate opening can be fit from the curvilinear fracture zones with 33 degrees of clockwise rotation.

**Rachel Clark***Sediment transport and accumulation in the Amundsen Sea, West Antarctica*

The marine-based glaciers draining into the Amundsen Sea today are experiencing a net loss in ice mass. This change comes about as the warm, Circumpolar Deepwater from the deep ocean flows onto the continental shelf and melts the glaciers at the ice front. In the past, this region has been under investigated due to prevailing sea ice conditions and poor weather. Two research cruise aboard the RV/IB Nathaniel B. Palmer travelled to this region in 2019 and 2020 to carry out geophysical surveys and collect marine sediment cores across the region. Over eighty sediment cores were collected to investigate glacial and oceanographic history and sediment dynamics. A subset of these cores was selected to investigate sediment accumulation rates primarily using  $^{210}\text{Pb}$  geochronology in the uppermost sediments that likely accumulated in the past 100 to 150 years. From this method, sub-centennial scale age models were created to investigate both history of sediment accumulation and changes in sediment accumulation rates. Additional sediment core proxies are used to give context to these rates, including grain size and shape data, computed tomography scans, magnetic susceptibility, and density. A facies classification has been applied to the observed sediment packages, which highlights the sediment transport processes for relevant for calculated sediment accumulation rates. Results show that there is a semi-constant accumulation of glacial marine mud, which is most likely sourced from subglacial meltwater escaping into the Amundsen Sea. This mud accumulates at a rate of 1 mm/yr across most of the region. However, there are noticeably higher rates at shallower sand/or more ice-proximal sites (up to 3.7 mm/yr), suggesting bathymetric features and proximity to the sediment source affect sediment accumulation. Data also imply that mass flow deposits are an important secondary process. The mass flow deposits vary in grain size and sedimentary structures, and they are not consistently found within all marine sediment cores. Finally, in some cores with high resolution  $^{210}\text{Pb}$  data, there is an observable slowing down in sediment accumulation near the ice front over the past century. Future work aims to isolate the mechanisms responsible for this observed slow down.

**Daniella Easley***Variations in the expellable potential of Late Cretaceous source rocks from Trinidad to Guyana: An evaluation of the influence of tectonic, paleogeographic, and global isotopic excursions on organic deposition and preservation*

The Ultimate Expellable Potential (UEP) of million-year intervals (acmes) was modeled for the Cretaceous source rock system in the hydrocarbon-rich areas of Trinidad and Guyana. Regional tectonics and basin development provide likely explanations for the observed similarities and slight differences between the source rock potential in the two regions that are separated along the trends of the late Cretaceous-Cenozoic passive margin of the Central Atlantic Ocean. During the Aptian-Albian, the Guyana margin experienced shearing along the Demerara transform fault related to the early Cretaceous opening of the Equatorial Atlantic Ocean. During the Middle Miocene, Trinidad area experienced fold and thrust deformation associated with collision between the passive margin in this area with the eastwardly-migrating Caribbean Plate. Using an updated approach to UEP modeling, both the variations in organic content of the source rock and the total thickness of the source rock sections are considered. To identify acme time intervals that represent significant organic deposition and preservation, the measured TOC and HI values for each sample were used to back-calculate the original TOC and HI at deposition. Inorganic parameters, such as S and  $\text{Al}_2\text{O}_3$ , were also used to differentiate organofacies of the source rock kerogen. The results of UEP modeling completed from ten individual wells in the Trinidad-Guyana-Suriname area show that the eight Late Cretaceous geologic intervals exhibit variable hydrocarbon potential, with the Coniacian sections exhibiting the highest and most consistent UEP across the study area. The patterns of organic deposition in Trinidad and Guyana also indicate similar transitions between organofacies B to A during the Santonian, coinciding with widespread basin flooding along the margin. While the two regions show similar patterns of source rock potential and a transition in organofacies at similar points in time, the Cenomanian-Turonian section shows minimal hydrocarbon potential in the Trinidad region and variable potential throughout the Guyana-Suriname Basin. We propose that source rock potential in both areas is unrelated to any global anoxic events, and more likely related to localized, paleogeographic variations along the single rifted-passive margin between Trinidad and Guyana.

**Md Nahidul Hasan***Estimating thermal stress and expelled hydrocarbons from Mesozoic-Cenozoic source rocks of southern Gulf of Mexico*

The Campeche and Yucatan salt basin along the southern Gulf of Mexico (GOM) remains one of the least explored areas of the GOM basin. This study uses a grid of 23,600 line-km pre-stack depth migrated (PSD M) 2D seismic reflection profiles, shipborne gravity data, and open-source geologic information to model the thermal stress of four potential source intervals (Oxfordian, Tithonian-centered, Ceno-Turonian, Lower Miocene). 1D thermal modeling of two margin-perpendicular transects each consisting of five pseudo wells that were integrated with mapping of the grid of seismic reflection data. This 1D modeling takes into account the thermal stress variations related to the depth of base lithosphere, crustal type and thickness, paleo-water depth, Jurassic salt thickness, and the transient, heat flow effects related to recent clastic sedimentation. The result of modeling was that deeply-buried, salt-related minibasins along the outer marginal trough predicts mature hydrocarbons which is also supported by the presence of natural oil seeps. Quantitative expelled hydrocarbon estimation shows that Oxfordian and Tithonian-centered source intervals generated 33 and 103 million bbl of oil equivalent [BOE]/km<sup>2</sup> in the outer marginal trough, respectively.



### James McConnell

#### *Distribution and thickness of sediment-filled rifts in the deep-water Camamu-Alamada rifted-passive margin of northeastern Brazil of northeastern Brazil*

The Camamu-Almada offshore sedimentary basin occupies 25,000 km<sup>2</sup> along the Atlantic coastline of northeastern Brazil. Explorationists have discovered commercial hydrocarbon deposits on the continental shelf, yet the deep-water zones of the Camamu-Almada basin remain largely unknown. I correlated a 17,840 km grid of offshore 2D seismic reflection lines. Using these data, I mapped basement-intersecting, normal fault-bounded rifts of Valagininian to Aptian age that were filled by inferred fluvial and lacustrine facies tracts. The zone of rift structures—half-grabens, grabens, and horsts—extended 120 km basinward of the coastline. Half-graben depocenters abutting the continental slope contained up to 3 km of pre-rift and syn-rift sediments with the largest rift basins reaching areas up to 500 km<sup>2</sup> in map view. The Cretaceous syn-rift section may host source-reservoir rock pairs in deep-water areas that are like those confirmed on the continental shelf. Such pairings would be analogous to elements of the shallow-water Morro Do Barro petroleum system(!). Rift half-graben seismic facies assemblages of chaotic, weakly parallel, and low amplitude reflectors adjacent to the bounding normal fault grading into parallel, higher amplitude reflectors away from the bounding normal fault was frequently observed in both the deep-water and shallow water zones. Said assemblage of seismic facies may represent a geologic facies tract consisting of both coarser-grained sediments favorable for reservoirs and fine-grained organic-rich lakebed source rock candidates. Seismic facies observed in the dataset support the notion that geologic facies present in rift half-grabens on the shelf and slope containing source-reservoir rock pairs are also present in the deep-water. The youngest syn-rift section—the Rio de Contas Formation—was recognized in half grabens across hyperextended continental crust terranes in the deep-water zone. Previous work showed lacustrine source rocks in the uppermost Rio de Contas Formation sit in the late oil window today (1.12 %Ro – Romito et al., 2021). The presence of syn-rift sediments in deep-water and their position in the late oil window indicate the presence of an outboard petroleum system.

### Claire Ong

#### *Analysis of PFAS in the Edwards Aquifer*

Poly- and perfluoroalkyl substances (PFAS) are highly resistant to degradation and may accumulate to levels above the EPA advisory limit (70 ng/L). Drinking water may provide a primary and direct source of PFAS to humans, and it is imperative to quantify and monitor PFAS in water sources, especially easily contaminated sources such as aquifer systems. 34 water samples collected from 19 different locations in the Edwards-Trinity Aquifer System (Texas) have been analyzed for 25 PFAS (C4-C10) using liquid chromatography mass spectrometry (LC/MS). C4-C8 PFAS have been detected with a notable prevalence in short-chain perfluorocarboxylic acids (PFCAs). Long-chain PFAS are more hydrophobic compared to short-chain PFAS and preferentially bind to sediments and other particles, while the short-chain constituents stay mobile in water. Considering the distance of the sample locations from urban areas, the short-chain PFAS may partially be attributed to the degradation of more volatile PFAS (such as PTOHs and FASEs), while both short and long chain may also have originated from the transformation of PFAS precursors (including PTSAs and PAPS). Origins of analyzed PFAS will be pinpointed and inferred based on typical recreational usage, distance to industrial and urban areas, distance to waste water treatment plants, and other common sources.

### Ruby Patterson

#### *In Situ Resource Utilization Potential of Artemis Landing Site 105, Lunar South Pole*

Human and robotic missions supporting NASA's Artemis Plan will initially target the lunar south pole and assess the nature and availability of ices for in situ resource utilization (ISRU) to facilitate a sustained exploration program. Here we augment previous studies of potential Artemis landing sites with an analysis of Site 105 (87.18° S, 62.84° E) and potential water- and dry- ice deposits in that area. A MoonTrek NAC mosaic with >1.25 m/pixel resolution was used as the base map for visual analysis. Surface roughness and slope were calculated from DEMs. Potential ISRU locations were determined using LOLA data in 120 m/pixel resolution. The Diviner data portal provided temperature data at a resolution of 240 m/pixel. Hydrogen abundance data was obtained from NASA PDS Geoscience Node in a spatial resolution of 0.5° by 0.5°/pixel. ISRU maps were resampled for a final map resolution of 240 m/pixel. Finished map products were created using ArcGIS Pro Version 2.6.0. At the spatial resolution (240 m/pixel) of our study, no regions exist within a 2 km radius of Site 105 where water- and dry- ice are stable in both summer and winter. Within 10 km, 14.77 km<sup>2</sup> (4.70% of radial zone) may possibly contain seasonal water-ice. The 20 km zone contains 196.25 km<sup>2</sup> (15.61%) of area suitable for water-ice stability and 0.95 km<sup>2</sup> for dry-ice. A small area of dry-ice stability is located just inside the rim of Faustini crater, is far from high illumination areas, and is only accessible through steeply sloping and rugged terrain. The seasonal nature of the potential deposits suggests any trapped volatiles will be dominated by solar wind and micrometeorite impacts.

**Muhammad Qasim**

*Integration of multispectral and hyperspectral remote sensing data for lithological mapping in Zhob Ophiolite, Western Pakistan*

This work integrates processed satellite-based remote sensing products and the laboratory data for the geological studies of the Naweoba block of Zhob ophiolite. This ophiolite is one of the north-south trending chain of ophiolite bodies obducted onto the Indian Plate during the collision of the Indian and Eurasian Plates. Lack of a complete accessibility to this area due to the prevailing law and order situation and economic mineral resources usually associated with ophiolite bodies gave a motivation to study the area using remote sensing techniques. Advanced Spaceborne Thermal Emission and Reflection Radiometer (SWIR) and Sentinel-2B reflectance data are processed using Decorrelation Stretch, Band Indices, Principal Component Analysis, and Minimum Noise Fraction. Each of these algorithms generated the products of varying accuracy for both the datasets because they have a different spatial resolution, 30m for ASTER and 10m - 20m for Sentinel 2B, and a varying number of spectral bands, ASTER have six Short Wave Infrared (SWIR) bands while Sentinel 2B have only two SWIR bands. Therefore, these remote sensing products are integrated for better discrimination of the lithological units of the Naweoba block. Six rock samples collected during brief fieldwork are analyzed in the laboratory for the spectral signatures using Analytical Spectral Device spectroradiometer and SPECIMS Hyperspectral SWIR camera. Diagnostic spectral absorption features of different minerals are used for lithological mapping of satellite images. A petrographic study of the field samples is also conducted to confirm the lithologies identified through the spectral signatures. The lithological map prepared in this study correlates well with the recently published geological map of the Naweoba block that had been prepared through conventional fieldwork methods. Based on the spectral signatures, corrections in the extension of some of the previously mapped ultramafic bodies are also made, along with the identification of some new peridotite exposures in the ophiolite that had not been mapped previously by the conventional field methods. Chert and basalt units identified in this block may have the potential for economic deposits of manganese. Additionally, chromite can be found in the peridotite and Rare Earth Elements (REEs) in the gabbro and plagiogranite of the Naweoba block of Zhob ophiolite.

**Kamil Qureshi**

*Structural Geometry and Lateral Propagation of the Surqamar Anticline, Northern Suleiman Fold-Thrust Belt, Western Himalayas*

The Manzai Ranges (part of northern Suleiman Fold-Thrust Belt) at the western margin of the Indian plate lies in the recess settings and provides a unique opportunity to study oblique margin structures related to compressional and transpressional tectonics and mechanisms of active fold growth. In the present research, 2D seismic data have been integrated with surface geological and geomorphological mapping to interpret their structural geometry as fault-bend, fault propagation, or detachment fold and their geomorphic evolution. The topographic expression of the Manzai Ranges is associated with the Khirgi, Jandola, Manzai, and Surqamar anticlines. Both the frontal anticlines (Manzai & Surqamar) have different geomorphic expressions i.e. the Manzai anticline is a low topographic ridge with steep forelimb evolving more as fault-propagation fold geometry. While northeast plunging Surqamar anticline has a very gentle surface expression as a detachment fold. Stream networks, drainage density, and elevation profiles are delineated using high-resolution digital elevation model to understand fold growth and its lateral propagation. Surqamar anticline shows active wind and water gaps, decreasing drainage density and dissection towards eastern segment with drainage deflection in the same direction. The transverse elevation profiles shows the mean elevation change along the Surqamar anticline. Hence, it shows lateral propagation of the structure in the northeastern direction. A 23 km long 2D seismic reflection data was used to constrain the geometry, depth to detachment, and amount of shortening across the frontal 20 km long Surqamar anticline. We interpreted Surqamar anticline as a detachment fold with detachment in the Paleocene age rocks at a depth of 4.1 km. We created Area-Depth graph following Fault Trajectory method to validate our interpretation, which matches our results giving a detachment depth and dip of 4.1 km and 2.5, respectively. The method calculates total shortening of 1.7 km across the Surqamar anticline with root mean square error of 96%. In addition, this method allow us to separate the timing of growth and pre-growth sequence. Our study will contribute better understand structural geometry and geomorphic evolution of laterally propagating fold in active tectonic setting of western Himalayas.

### **Juan Pablo Ramos**

#### *Coniacian-Santonian-sourced petroleum system along the deepwater Caribbean margin of Colombia*

The deepwater Caribbean margin of Colombian remains an underexplored frontier with no significant hydrocarbon production despite exploration and wildcat drilling over the past decade. For this study, I integrated well data from the DSDP program with seismic reflection data to better understand the potential of previously documented Coniacian-Santonian rocks with very good organic content (average TOC of 3.7% and maximum values of 11.4%). A Rock-Eval Analysis of samples from this interval in recent years showed that these sequences were immature at the DSDP sites. However, this observed immaturity of the source can be explained by the location of the DSDP wells on structural highs located hundreds of kilometers north of the much deeper buried Colombian margin. In order to document this source rock interval along the Colombian margin, I will show a variety of Direct Hydrocarbon Indicators (DHIs) that include prominent and continuous bottom-simulating reflectors, cross-cutting reflectors, dimmed intervals, bright spots, and gas chimneys that can be shown in many cases to emanate from the well-mapped Coniacian-Santonian source rock horizon. The presence of widespread DHIs combined with the correlation with the DSDP wells on structural highs allows me to propose the presence of an active petroleum system over large areas of the Colombian Caribbean margin. Additionally, I will show examples of widespread potential traps that include: 4-way structures of the Southern Caribbean Deformed Belt deformation front and stratigraphic traps related to channel-levee complexes and turbidites. Both trap types contain high-porosity, sandy reservoir sandstones deposited in submarine channels of the Magdalena Fan System. An important point concerning my proposed petroleum system is its location on the subducting Caribbean plate rather than the overriding Colombian deepwater margin which has been the main focus of previous offshore exploration and wildcat drilling.

### **Aydin Shahtakhtinskiy**

#### *Quantifying the impact of Hurricane Harvey on barrier island systems of the Central Texas Coast and their recovery: an example from Mustang Island*

In the past two decades (2001–2020), Texas has experienced an increase in the number of tropical storm and hurricane landfalls, including most recently by Hurricane Harvey. Studying the erosional effects of past storms is important for preparation for future storms and protection of ecosystems and recreational sties. This study used datasets downloaded from public domains and covering the Mid Texas Coast, including 1-m spatial resolution bare-earth digital elevation models (DEMs) derived from airborne lidar acquisitions before (2016) and after (2018) Hurricane Harvey used for quantitative analysis of change, and several sub-meter scale orthoimages pre- and post-Harvey used for qualitative analysis. Shoreline proxies were extracted to quantify shoreline retreat and/or advance, and DEM differencing was performed to quantify net erosion and/or deposition. Initial analyses show retreat of the shoreline and significant level of erosion of the beach elements immediately after Harvey landed (August–September 2017). While foredune ridges act as first-level buffers against the impact continuously along the coast, this erosion proceeds to back-barrier areas via inlets/passes. 2018 data show that within nine months after the hurricane, the barrier-island systems have started recovering towards their initial position. It is also observed that local depositional events can significantly add to this recovery. Future work includes analysis of post-storm dune changes, including their sizes and rates of erosion or retreat. Additionally, an unmanned aerial vehicle (DJI Matrice 600 Pro) and structure-from-motion photogrammetry will be used to produce a three-dimensional photorealistic model of the dunes and cm-scale DEM and orthoimage of a selected site at Mustang Island. These products will be used to describe the dune geometry and morphology in more detail and the current state of the beach. This study aims to enhance the understanding of major storm impacts on coastal areas and help in future protection planning of the Texas Coast.

### **Ozzy Tirmizi**

#### *Hazard Potential in Southern Pakistan: A Study on the Subsidence and Neotectonics of Karachi and Surrounding Areas*

Coastal communities in deltaic regions around the world are subject to subsidence through a combination of natural and anthropogenic processes. The city of Karachi in southern Pakistan is situated along the diffuse western boundary of the tectonically active Indian Plate and is susceptible to earthquakes and faulting, along with anthropogenic processes such as excessive abstraction of groundwater and upstream construction of dams and barrages. Few previous studies in the area and lack of historical data make it difficult to determine the rate of deformation and the individual contributions from each factor. We present an integrated study of the subsidence and neotectonic activity of Karachi and its surrounding areas using static GPS survey data and Interferometric Synthetic Aperture Radar (InSAR) time-series techniques to determine the severity and extent of deformation. Positional time-series analysis of the static GPS survey data reveals a displacement of approximately 3.25 cm in the north direction, 3.8 cm in the east direction, and 0.2 cm down in the vertical direction per year from 2006 to 2016. The InSAR results for satellite LOS velocity change in both ascending and descending tracks indicate movement away from the satellite in key residential and industrial areas. Further decomposition into 2 dimensions (east-west and vertical) quantifies displacement in these areas to about 1cm to  $\geq 3$ cm downward per year from 2015 to 2020. Karachi is one of the most densely populated cities in the world, with an estimated population of over 16 million people. Determining the rate of subsidence and extent of neotectonic activity is crucial for mitigating seismic hazard.

**Ana Vielma***Distribution of trace elements inside source rocks*

Trace elements in sedimentary organic matter have been used in various fields such as paleoenvironmental studies, geothermal exploration, and petroleum systems analysis. For petroleum exploration and exploitation, the use of trace elements has been applied extensively in source-oil fingerprinting, thermal maturity assessment, and source-rock characterization, among other areas. However, there are still many uncertainties about their use, due to procedural and instrumental limitations which challenge their quantification, because they are present in very small amounts. Another complication is related to the analysis of organic molecules which have the capability to coordinate and form complex structures difficult to isolate and interpret. Therefore, there is little detailed understanding of the distribution of trace elements inside organic-rich source rocks. Since bitumen is used as a laboratory proxy of the oil that has migrated from a specific source rock, this work measures the abundance of trace elements in whole rock and its equivalent extracted rock (solvent-washed rock) to estimate their abundance in bitumen. This research evaluates the impact of organic-solvent washing in the remobilization of trace elements out of the organic-rich rock. Additionally, this work also tested the repeatability of a novel methodology recently developed at UH that seeks to achieve a complete elemental recovery and removal of metals in organic matrices with good levels of precision and accuracy. This work utilizes the high accuracy and precision of the investigated method for rocks analysis. Most of the analytes are reproducible with a precision in elemental abundances lower than 5% (relative). Once the reproducibility of the method was satisfactorily tested in organic-rich source rocks, trace elements in extracted rocks were analyzed. Several aliquots of each sample were exposed to Soxhlet extraction to obtain washed rocks (extracted rocks). After quantification of the abundance of trace elements in extracted rocks, it was possible to develop a model to infer the abundance of trace elements in their equivalent bitumen. Future work will investigate the accuracy of this model by quantifying the abundance of trace elements in the extracted bitumen and comparing the real values versus the predicted ones.

**Nina Zamanialavijeh***High-velocity slip during thermal decomposition of carbonates: example from the Heart Mountain Slide ultracataclasites, Wyoming*

Frictional in carbonate rocks leads to breakdown of carbonate minerals upon heating and production of gaseous CO<sub>2</sub>. Several physical and chemical processes strongly affect friction during motion along slip surfaces in faults and landslides. Grain size reduction (comminution) and the increase in pore pressure related to gas expansion drastically lower the strength of the cataclastic material. The temperature at which these processes take place is critical to evaluate the mechanical behavior of these slip surfaces. Here, we first review previous observations on natural and laboratory deformed carbonates and provide additional information from the Heart Mountain Slide, Wyoming, a gigantic gravity slide. The new observations based on static thermal experiments, magnetic data and petrographic observations, indicate that, at shallow depths, thermal decomposition begins at ~400°C, significantly lower temperature than previously thought. These results suggest that the frictional behavior of fault rocks in carbonates may need to be revisited.

**Ph.D. GEOPHYSICS****Christopher Calvelage***Earth's wandering rotation axis influenced by mantle convection*

Paleomagnetic measurements show that the magnetic poles have moved over geologic time with respect to tectonic blocks. This is known as Apparent Polar Wander, as it can be explained by the relative motion of tectonic plates. A portion of it, however, can only be explained as a motion of the lithosphere as a whole with respect to the magnetic poles, and it is thus called True Polar Wander (TPW). This process depends on large scale mass redistributions, either on the Earth's surface or within the mantle, that perturb the Earth's moment of inertia. One large scale mechanism that can change the distribution of mass within the mantle is the process of mantle convection. Due to recent advances in reconstructions of past plate motions and in the theory of geodynamic retrodictions, we can calculate explicitly past mantle states and use them to predict TPW back in time. Such predictions are subject to a number of geological and geodynamic assumptions, such as the distribution of past subduction zones and the viscosity of the Earth's mantle. We can thus test these assumptions by comparing the predicted TPW histories to paleomagnetic observations. Preliminary results suggest this method is effective for constraining mantle convection states through time.

**Otto Gadea***Detection of Bastnäsite-Rich Veins in Rare Earth Element Ores through Hyperspectral Imaging*

Spectral indices are a well-established remote sensing tool that has been showcased in many studies pertaining to different fields such as agriculture, forest ecology, geology, soil sciences, vegetation, water resources, and urban development. In the case of geology, several indices already exist for the purpose of highlighting regions with interesting lithologies, such as iron oxides, aluminous clays, carbonates, and mafic to ultramafic minerals, based on signature absorption features in their reflectance spectra. However, in the literature, most indices often depend on the very few, wide spectral bands used by airborne or spaceborne multispectral imagers such as Landsat 8 OLI, Terra ASTER, and Sentinel-2 MSI. Hyperspectral imagers are able to glean more detailed compositional information of a rock surface by operating with a myriad of narrow spectral bands, though the usage of these bands in spectral indices for mining and exploration purposes remains largely unexplored. We propose a new Bastnäsite Index (BI) capable of detecting the presence of rare earth elements (REEs) and mapping their relative abundances across rock surfaces.

**Veronica Guzman***Stress Variations in the Delaware Basin from Shear-Wave Splitting Analysis*

Seismicity in the Delaware Basin has been experiencing a sharp increase since 2009, attributed to wastewater injection and hydraulic fracturing. In the past two years, several relatively large induced earthquakes occurred in Culberson County in the northwestern part of the basin, including an M5.0 earthquake in March 2020. It is critical to investigate variations of stress in the area in order to better understand the development of induced earthquakes. Shear-wave splitting (SWS) is caused by the preferred alignment of induced cracks, and the fast polarization orientation indicates the maximum horizontal stress direction in the upper crust. However, the increase of pore pressure could alter the crack alignment and change SWS parameters. SWS has been used to map stress and pore pressure changes to analyze induced seismicity. This study aims to identify spatial and temporal variations of stress or pore pressure in the Delaware Basin by measuring SWS parameters. We have processed over 4,000 seismograms from local earthquakes since November 2019 at five TexNet seismic stations (PB09, PB28, PB28, PB31, and PB33) and obtained the fast directions and delay times. The average fast polarization orientations are consistent with fault systems or maximum horizontal stress. Temporal analysis of parameters from the longest-lived station in our study revealed the emergence of large angle orientations after the M5.0 earthquake, suggesting an increase in pore pressure that leads to fault slip in orientations less favorable to the existing stress field.

**Chesney Petkovsek***Mechanism to explain lateral variations in the geothermal gradient of the Delaware Basin, West Texas, as measured and calibrated from 1024 deep exploration wells*

Previously proposed ideas for explaining variations in the geothermal gradient of the Delaware Basin include 1) localized heating from Eocene-Miocene intrusive rocks along the western margin of the basin; 2) heating from radiogenic decay of minerals within Proterozoic sialic intrusive rocks within the Proterozoic crystalline basement underlying the entire basin; 3) the rise of hot fluids from thick-skinned and deeply-buried fault zones within the Proterozoic basement underlying the basin, and 4) uniform heating of the entire basin deep burial by Laramide foreland basin clastic rocks of Late Cretaceous-Eocene age have now been eroded from the Laramide orogeny to the west of the basin. To test which of these mechanisms is most important for explaining variable gradients in the Delaware Basin, I compiled raw, bottom-hole temperatures (BHT) from 1024 deep well logs (>17,000 TVD), from which I derived four stratigraphic interval-specific geothermal gradients for which were corrected using mean surface temperature and the Horner relation. Based on this map of corrected gradients, the results of the study include 1) the area of the xx-km-wide Abilene gravity minimum (AGM) - that has been inferred to be an area of thicker Proterozoic sedimentary rocks forms an east-west zone of lower gradients; 2) gradients over Proterozoic mafic intrusive rocks that flank the AGM to the north and south are lower than gradients overlying rhyolitic or granitic areas, and 3) higher gradients at the higher stratigraphic level (Ochoan to the surface) and elongate and parallel the east-west trending Grisham fault. My two proposed primary controls on heat flow in the Delaware Basin (more sialic intrusive rocks; upward fluid flow from basement fault zones) can explain the non-uniform variations between burial and source rock maturation and the large spatial variations in gas-to-oil ratios within drilling intervals within the Delaware Basin.

**Sara Rojas***Quantifying Vegetation and Land Cover Changes about the Path of Hurricane Harvey*

Hurricane Harvey made landfall as a category 4 hurricane near Rockport, Texas on August 26th of 2017. This study presents a preliminary analysis of both regional- and local-scale vegetation changes in affected Texas areas. By utilizing the Normalized Difference Vegetation Index (NDVI), changes to vegetated areas can be examined by comparing the ratio of reflected near-infrared to red light visible in multispectral imagery. NDVI values range from -1 to 1, where water bodies are represented by negative NDVI values. Unfortunately, there are no distinct NDVI boundaries for each land cover class. High NDVI values typically represent dense or healthy green vegetation, and lower positive values commonly represent barren lands, stressed vegetation, or even urban areas. Therefore, this study aims to develop a method to quantify the severity of vegetation changes moving away from the immediate path of the hurricane, using Landsat-8 imagery and The National Land Cover Database (NLCD). The extent of land cover change and vegetation health was also examined based on distance from the shoreline, focusing particularly on coastal beaches and vegetated dune areas. In conclusion, this work provides information on vegetation health and density in coastal areas, vegetation recovery times, and land cover types particularly susceptible to storm damage, such as cultivated crops, barren lands (beach areas), and wetlands. Overall, this work explored strategies used to quantify changes caused by hurricanes and tropical storms. By using a recent event, the methodology can be perfected before applying it to twenty years' worth of tropical storm and hurricane data in future work.

**Kenneth Shipper***Testing rift versus transform models for the Guyana margin using 3D gravity model in contrast to seismic reflection data*

The 700-km-wide Guyana margin of northeastern South America includes a 40-50 km thick elevated Archean greenstone belt of the Guiana shield that thins to a 26-11-km-thick necked zone of continental crust which thins to normal 9-6-km-thick oceanic crust. To the east, Suriname is partially fronted by a volcanic margin composed of Middle Jurassic volcanic flows underlying the Demerara Plateau. The Jurassic tectonic origin between the Guyana-Suriname margin remains controversial with two, widely differing models for its tectonic origin: 1) the margin formed along a Jurassic transform related to the early opening of the Central Atlantic Ocean; 2) the margin formed by orthogonal rifting related to the Jurassic opening of the Central Atlantic. To test the two models, we perform a 3D gravity inversion with marine satellite gravity constrained by previous refraction surveys and a grid of 2D seismic data. Margin-perpendicular transects from the inversion exhibit a 167-74 km tapered necked zone with an average top basement gradient of 4 degrees supporting a rifted-passive origin. This thinning, wide necking zone, and the location of the continent-ocean boundary has a significant impact on the heat flow across the margin.

**Larkin Spires***Observations from Empirical Fluid Substitution in Shales: Why Use the Voigt-Reuss-Hill Average?*

New investigation shows limitations in using the Voigt-Reuss-Hill average in certain lithologies. The Reuss bound represents the effects of a suspension or a horizontally layered media on the bulk modulus while the Voigt bound represents vertical layering that resists compression via the strongest components. In using Brown and Korringa for fluid substitution in seven shale formations, a parameter,  $\beta$ , was used to weight the Voigt and Reuss averages to approximate the bulk modulus of the mineral matrix. In six of the seven shale formations, the optimal fit occurred at or near the Reuss bound. To study the reasonableness of this result, fluid substitution was performed on the individual layers of a synthetic aggregate rock consisting of homogenous, non-communicating layers of clean sandstone and kerogen with Gassmann's fluid substitution from brine to 70% gas saturation. The results from the individual layers were averaged to represent what a logging tool would measure for porosity, density, and velocity. The results for the aggregate synthetic rock were compared to fluid substitution using different  $\beta$  values in the calculation of the bulk modulus. The results closest to the modeled result occurred when bulk modulus equaled the Reuss bound.

# TO ALL OF THIS YEAR'S PRESENTERS





*Madeline Statkewicz*

**STUDENT RESEARCH CONFERENCE CHAIR & CONTENT CREATOR**

I am a fourth-year Ph.D. candidate in atmospheric science working under the advisory of Dr. Bernhard Rappenglueck. Hailing from Mobile, AL, I earned my B.S. in applied mathematics and minor in physics from the University of South Alabama. My work investigates the changing nature of precipitation events, local atmospheric circulations like the land-sea breeze, the rapidly expanding built environment, and their intersections. In my free time, I love painting, hand embroidery, DIY projects, and my gray cinnamon cockatiel, Pascal.



*Michael Martinez*

**ASSISTANT CONFERENCE CHAIR & JUDGING COORDINATOR**

I am a second-year M.S. student in Geology working under Dr. Lorenzo Colli and Dr. Alexander Robinson. Previously, I earned my B.S. in Geology at Texas A&M University, where I first developed my interest in exploration geoscience. My current work focuses on the Late Cenozoic uplift and tilting history of the U.S. Midcontinent using numerical lithospheric flexure modeling. I hope my work contributes to understanding more about continent-scale mantle dynamics and flexure in North America through computational methods and geologic observations.



*Ana Vielma*

**ASSISTANT JUDGING COORDINATOR**

I am a Ph.D. Candidate under the supervision of Dr. Bissada and Dr. Casey. I graduated with honors as a B.S. in Geological Engineering from Los Andes University in 2009. My research interests are broadly in the field of petroleum geochemistry. My dissertation aims to get insights over trace elements interaction between the organic fractions + inorganic matrix of organic-rich source rocks which is critical for paleoenvironmental assessments, thermal maturity, and petroleum systems analysis in general. Besides my scientific interests, some of my hobbies are related to outdoor activities, playing saxophone, reading, yoga, meditation, and dancing Latin music.



*Veronica Guzman*

**NSMIT Liaison**

I'm currently a second year Ph.D. student working under the supervision of Dr. Aibing Li. I completed my M.S. and B.S. at the University of Houston. My current research is based on analyzing induced seismicity in the Permian Basin through shear-wave splitting measurements. My current work focuses on automating the shear-wave splitting measurement workflow and integrate the splitting parameters with injection data to determine earthquake mechanisms and analyze any temporal stress or pore pressure changes. This work will have impact on seismic hazard assessments and the monitoring of wastewater disposal and hydraulic fracturing activities.





*Morshad Ahmed*

**ASSISTANT TO NSMIT LIAISON**

I am a third-year Ph.D. student in atmospheric science working under the supervision of Dr. Bernhard Rappenglueck. Previously, I earned my B.S. in Chemistry and M.S. in Inorganic and Analytical Chemistry at the University of Dhaka, Bangladesh. My work focuses on the sources and photochemical behavior of atmospheric pollutants (nitrophenols, mercury, and non-methane hydrocarbons) in Houston which will help mitigate air pollution, thereby improving air quality and public health. My hobbies include playing cricket and traveling.



*Sara Rojas*

**ORGANIZATION OF MATERIALS**

I'm currently in my first semester as a Ph.D. student in Geophysics, working under the advisory of Dr. Shuhab Khan. I completed my undergraduate degree, B.S. in Physics, at the University of Houston. My research focuses on quantifying episodic, annual, and decadal changes to Texas beach-dune systems over the last twenty-two years. Using different components such as shoreline change, sediment volume, vegetation health and density as an analog for beach-dune resiliency, I'm attempting to quantify the impact of hurricanes and tropical storms, oversee recovery, and discern what characteristics may regulate an area's resiliency. This work could assist in further identifying at-risk coastal regions and provide state and local agencies with time- and cost-efficient coastal rehabilitation strategies.



*Tanzina Akther*

**ORAL SESSION HOST**

Currently, I am in the second year of my PhD program at the Department of Earth and Atmospheric Sciences under the supervision of Dr. Bernhard Rappenglueck. My undergraduate and graduate degrees are in Chemistry, from the University of Dhaka, Bangladesh. Specifically, my research focuses on ozone precursors and how that varies with planetary boundary layer heights. As part of my PhD, I will investigate the sources of resolved and unresolved reactive organic carbon's emissions from different sources. The results of this study will allow the government to take the proper mitigation measures to reduce the emission of ozone precursors. Dancing, Zumba, and organizing are among my favorite things to do.



*Tabitha Lee*

**ORAL SESSION HOST**

I am a second-year Ph.D. student in atmospheric science working under the advisory of Dr. Yuxuan Wang. Previously, I earned my B.S. in environmental sciences with a concentration in atmospheric sciences at the University of Houston. My work concerns identifying and quantifying unreported NO<sub>2</sub> hotspots in satellite datasets. I hope my work can increase the societal benefit of satellite observations and allow for overlooked or remote locations to have their air quality assessed.

We would like to thank all who volunteered as judges for this event, whether from EAS faculty and staff, industry guests, University of Houston Alumni, or some combination therein. The Student Research Conference would not be what it is without you!

<b>1</b>	Irene Arango	<i>Chevron</i>
<b>2</b>	Elizabeth Baker	<i>Shell</i>
<b>3</b>	Humberto Carvajal-Ortiz	<i>Core Laboratories</i>
<b>4</b>	Fernando Castillo	<i>Q-Spectrums Solutions</i>
<b>5</b>	Lorenzo Colli	<i>EAS Faculty</i>
<b>6</b>	Sharon Cornelius	<i>EAS Faculty</i>
<b>7</b>	Aya El Attar	<i>ConocoPhillips</i>
<b>8</b>	Rosemarie Geetan	<i>Bifrost Energy</i>
<b>9</b>	Gary Guthrie	<i>Roxanna Oil</i>
<b>10</b>	Stephanie Hari	<i>Hess Corporation</i>
<b>11</b>	Xun Jiang	<i>EAS Faculty</i>
<b>12</b>	Lillian Jones	<i>Geophysical Society of Houston</i>
<b>13</b>	Chinaemerem Kanu	<i>Jasco Applied Sciences</i>
<b>14</b>	Sanja Knezevic Antonijevic	<i>Occidental</i>
<b>15</b>	Klaas Koster	<i>Occidental</i>
<b>16</b>	Kristie McLin	<i>ConocoPhillips</i>
<b>17</b>	David Meaux	<i>BP, Retired</i>
<b>18</b>	Javier Miranda	<i>DeGolyer &amp; MacNaughton</i>
<b>19</b>	Duane Pierce	<i>Black Stone Minerals, Retired</i>
<b>20</b>	Mark Richardson	<i>ExxonMobil, Retired</i>
<b>21</b>	Minako Righter	<i>EAS Faculty</i>
<b>22</b>	Jinny Sisson	<i>EAS Faculty</i>
<b>23</b>	Linda Stembach	<i>Star Creek Energy</i>
<b>24</b>	Robert Stewart	<i>EAS Faculty</i>
<b>25</b>	Jiajia Sun	<i>EAS Faculty</i>
<b>26</b>	Ny Riavo Voarintsoa	<i>EAS Faculty</i>
<b>27</b>	Ye Wang	<i>ConocoPhillips</i>
<b>28</b>	Yingcai Zheng	<i>EAS Faculty</i>



We would also like to thank and acknowledge the College of Natural Science and Mathematics for their contributions to the 2022 Student Research Conference. Thank you for your support!

U N I V E R S I T Y of  
**HOUSTON**

---

COLLEGE of NATURAL SCIENCES & MATHEMATICS

# WHO ARE WE?


The Department of Earth and Atmospheric Sciences at the University of Houston has a wide range of research programs central to the earth sciences.

Air Pollution	Isotope Geochemistry
Air Quality	Marine Geology
Applied Geophysics	Micropaleontology
Applied Rock Physics	Potential Fields
Atmospheric Science	Remote Sensing
Carbonate Petrology	Sedimentology
Climatology	Seismology
Geodynamics	Sequence Stratigraphy
GIS	Structural Geology
Hydrology	Tectonics
Igneous Petrology	Thermochronology
Inorganic Geochemistry	Whole Earth Geophysics

The Department offers M.S. and Ph.D. degrees in Geology, Geophysics, and Atmospheric Sciences, a B.S. in Geology, Geophysics, and Environmental Sciences, and a B.A. in Earth Sciences. Fieldwork is a major component of all degree programs. The Department also offers Professional M.S. programs in Petroleum Geology and Petroleum Geophysics that are offered at convenient hours for professional geoscientists working in industry or aspiring for a professional position within the petroleum industry.

## CONTACT US

Department of Earth and Atmospheric Sciences  
4800 Cullen Boulevard, Houston, TX 77204

 (713) 743-3399

 <http://www.eas.uh.edu>